Theoretical studies on bioaerosol particle size and shape measurement from spatial scattering profiles

Chunxia Feng (冯春霞)[1,2], Lihua Huang (黄立华)[1], Jianbo Wang (王剑波)[1,2], Yongkai Zhao (赵永凯)[1], and Huijie Huang (黄惠杰)[1*]

[1] *Shanghai Institute of Optics and Fine Mechanics, Chinese Academy of Sciences, Shanghai 201800, China*

[2] *Graduate University of Chinese Academy of Sciences, Beijing 100049, China*

[*] *Corresponding author: huanghuijie@siom.ac.cn*

Received March 22, 2011; accepted April 4, 2011; posted online June 16, 2011

A method of clarifying bioaerosol particles is proposed based on T-matrix. Size and shape characterizations are simultaneously acquired for individual bioaerosol particles by analyzing the spatial distribution of scattered light. The particle size can be determined according to the scattering intensity, while shape information can be obtained through asymmetry factor (AF). The azimuthal distribution of the scattered light for spherical particles is symmetrical, whereas it is asymmetrical for non-spherical ones, and the asymmetry becomes intense with increasing asphericity. The calculated results denote that the 5°–10° scattering angle is an effective range to classify the bioaerosol particles that we are concerned of. The method is very useful in real-time environmental monitoring of particle sizes and shapes.

OCIS codes: 290.5850, 290.1090.

doi: 10.3788/COL201109.092901.

The field of biological agent detection has recently received considerable interest due to the high risk it poses to personnel even at extremely small amount of agent dose[1−3]. As a consequence of the high degree of lethality, it is essential to develop a new method that is especially sensitive to biological agents. It must be capable of detecting low levels or even single particle agents.

Among the many particle characterization techniques, optical methods offer genuine real-time non-destructive particle analysis and are highly cost effective. Fluorescence emission by particles is mainly used to discriminate between biological and non-biological particles[2,3]. Simultaneously, the magnitude or the total scattering intensity of the elastic light scattering can be used to determine the particle size[4−6], while the rate of generation of the light pulses can be related to particle number and particle concentration within the sampled atmosphere[7]. However, a further problem arises from the fact that biological agent particles have similar size and fluorescence characteristics, but different morphology cannot be differentiated. Therefore, particle shape proved to be a more effective method to discriminate between airborne particles of different types. Since the spatial pattern of the scattered light contains particle shape information[8], further analysis of the elastic light scattering may be effective in classifying aerosol particles by their shapes.

The T-matrix method is one of the most versatile, efficient, and widely used theoretical technique for computing the light-scattering properties of nonspherical particles based on the solution of Maxwell's equations. The T-matrix can be considered as a transfer matrix, which transforms incoming electromagnetic wave into scattered electromagnetic wave[9]. The T-matrix can be applied to the analysis of electromagnetic scattering by homogeneous and composite particles, clusters of particles, discrete random media, and particles in the vicinity of an interface separating two half-spaces with different refractive indices[10]. This approach has been applied to simulations of, for example, the optical properties of *Bacillus subtilis* spores, biconcave red blood cells, and living bacterial cells[11−13], as well as soot clustered agglomerates[14]. Several experiments have also been devoted to the field of single-particle spatial light scattering[15,16]. However, only few researches have referred to the shape analysis of biological agents, which is the subject of this letter.

One of the problems with the characterization of bioaerosol lies in determining their exact refractive index. For homogeneous biological cells, the refractive index $n = n_{\rm r} + {\rm i}n_{\rm i}$ is treated as a constant within the cells, where $n_{\rm r}$ and $n_{\rm i}$ are the real and imaginary parts of the refractive indx, respectively. Since different bioaerosols have similar compositions, we estimate their refractive indices to be the same. The typical refractive indices $n_{\rm r}$ of *Bacillus subtilis* spore range from 1.51 to 1.54 at $\lambda = 0.589$ μm[12], thus 1.52 and 0.017 are chosen as the real and imaginary parts of the refractive index of bioaerosol, respectively[17].

The manner in which a particle spatially scatters incident light is a complex function of the size, shape, composition, and orientation of the particle, as well as of the properties of the illuminating radiation (wavelength, polarization)[18]. As depicted in Fig. 1, the particle situates with the semi-major axis along the positive y axis of the laboratory coordinate frame, and it is illuminated with the circularly polarized beam directed along the z axis and perpendicular to the y axis. This is an important attribute that the particles display in actual measurement[15]. We assume that the refractive index of the particle in the sample is known and uniform, which is true in most cases. In this way, the scattered light intensity is only a function of scattering angle, particle shape, and particle size[19,20]. Then through analysis of the angular scattering pattern, the particle size and shape can be theoretically obtained[21−24]. In this letter, spherical and ellipsoidal models are used to investigate individual

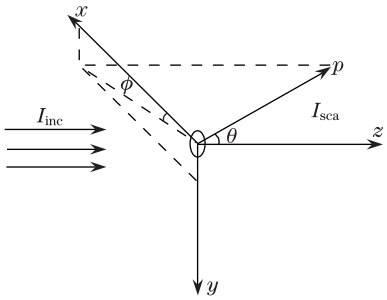

Fig. 1. Particle scattering geometry. θ: scattering angle measured from the positive z axis; ϕ: azimuth angle measured from the positive x axis in the clockwise sense when looking in the direction of the positive z axis; I_{sca} and I_{inc}: scattering and incident light intensities, respectively.

spherical and aspherical biological aerosol particles based on the T-matrix, which may provide theoretical basis in the rapid detection of harmful microbes in the air.

To facilitate the comparison, scattering results have been recorded for a wide variety of particle types, including spherical and non-spherical geometries. The spatial scattering by an individual particle may be described in terms of both the polar scattering (namely 0°–180° scattering in a plane containing the axis of the incident beam) and the azimuthal scattering (namely 360° around the axis of the incident beam at a fixed scattering angle).

The gray-scale images in Fig. 2 illustrate the spatial scattering intensity of individual polystyrene latex (PSL) particles of different shapes. The equal surface area radius is 1 μm, and the aspect ratios are 1, 0.8, 0.6, and 0.4, respectively. In each pattern, the origin point corresponds to 0° scattering, while the extreme circumference of the patterns corresponds to 90° scattering. The complete scattering pattern consists of a huge number of spots that represent a fingerprint of the specific morphology on the scatterer.

The scattering pattern in Fig. 2(a) shows that the profile distribution of the PSL sphere is symmetric. For any non-spherical particle, there is a non-uniformity of scattering intensity with the azimuth angle, and the asymmetry becomes intense with increasing asphericity, as can be clearly seen in Figs. 2(b), (c), and (d). As can be seen in Fig. 2, the intensity distributions are profoundly affected by particle shape. Thus, by analyzing the azimuthal distribution of the scattered light from one or a few particles, the particle shape information can be obtained. In this case, ellipsoidal particles with high aspect ratio can be distinguished from spherical ones using the azimuthal scattering patterns.

A simple and convenient method of processing spatial scattering data to yield particle shape classification indices is through the use of asymmetry factor (AF)[4,15]. AF is an assessment of the particle shape derived from the root mean square variation of the scattered light intensity around the scattering angle. It is calculated with data of different azimuthal angles around the specified scattering angle. This is expressed as

$$\mathrm{AF} = k\left[\sum_{i=1}^{m}(\bar{I}-I_i)^2\right]^{1/2}\Big/\bar{I}, \qquad (1)$$

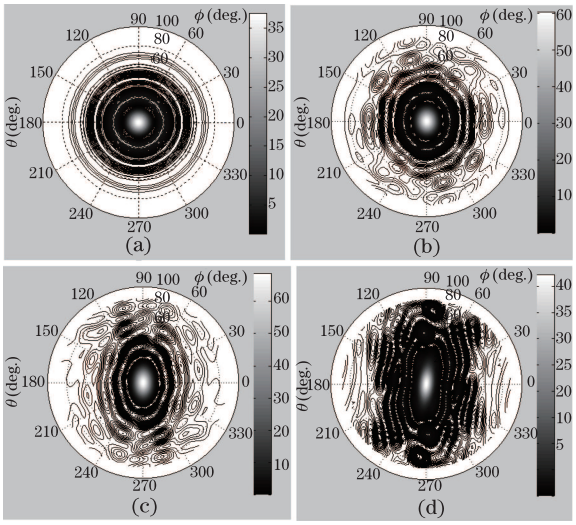

Fig. 2. Spatial scattering intensity generated by individual PSL particles of differing shapes. The equal surface area radius is 1 μm, the aspect ratios are (a)1, (b)0.8, (c)0.6, and (d)0.4; the scattering angle range is 0°–90°.

where m is the number of azimuthal data around the specified scattering angle, I_i is the scattering intensity corresponding to i around the specified scattering angle, $\bar{I}$ is the mean of all I_m values, and k is a constant to render the maximum possible value of AF to be 100, k=100/$\sqrt{m(m-1)}$. Therefore, perfectly spherical particles have AF = 0, whereas non-spherical particles have an AF ranging from 0 to 100[4].

Figure 3 shows the AF versus the scattering angle θ plots for individual PSL particles with the same size and shape as those in Fig. 2. It is clear that all the curves are monotonous in the 0°–15° scattering angle and that AF values increase with increasing non-sphericity. Thus, by selecting the optimum section of the scattering angle, the shape information can be obtained through the analysis of the azimuth fluctuations. Through the simulation of different particle sizes and shapes, we find that the first peaks of the distribution curves shift to the left or right. As the particle size increases, the first linear region narrows down accordingly. In order to improve the detectable upper limit of the particle size, the upper limit angle should not be too large. Considering the size and shape effect of different particles, we select the 5°–10° scattering angle as the optimum section and it proved to

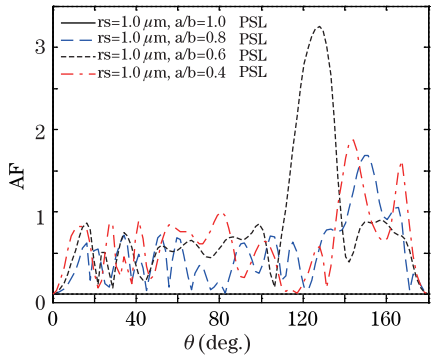

Fig. 3. AF versus θ plots for individual PSL particles with the same size and shape as those in Fig. 2. rs: sphere radius; a/b: aspect radio.

be appropriate for most particles.

Figure 4 shows the integrated scattering intensity in the 5°–10° scattering angle versus the azimuth angle (ϕ) plots for a variety of aerosols: *Staphylococcus*, *Yersinia pestis*, *Shigella dysenteriae*, and PSL particles. *Staphylococcus* is a coccus with sphere radius (rs) of 0.8 μm. *Yersinia pestis* and *Shigella dysenteriae* are both prolate ellipsoids in shape with a semi-major axis of 1.1–1.3 and 2–3 μm and a typical aspect ratio (a/b) of 0.75 and 0.35, respectively. They are similar in equivalent sizes but different in shapes. The PSL particles adopted are also spherical particles with radius of 1 and 1.3 μm.

The results suggest that spherical particles produce an equal response in all azimuth angles within a specified scattering angle. The scattering intensity is comparatively large for larger equivalent size particles, which means that the differentiation of spherical particles can be made by scattering intensity alone. In the case of non-spherical particles, the scattering intensity gives peak outputs at 90° and 270° azimuth angles (refer to the long axis directions of the non-spherical particles). It is this spatial scattering information that provides the particle shape classification. However, the scattering intensity of the *Yersinia pestis* and *Shigella dysenteriae* particles are not the same even if they have identically equivalent size, which might be attributed to the influence of the non-sphericity as well as the derivation approach of the equivalent size. Furthermore, the intensity fluctuation is aggravated by the increase in non-sphericity. The fluctuation of scattering intensity in the 5°–10° scattering angle with azimuth angle is evidently aggravated as the non-sphericity increases for the *Yersinia pestis* particle of low aspect ratio and the *Shigella dysenteriae* particle of even lower aspect ratio. Thus, by analyzing the azimuthal distribution of the scattered light, the particle shape information can be obtained. In this case, ellipsoidal particles with high aspect ratios can be distinguished from spherical ones using the azimuthal scattering patterns. In actual measurement to realize particle size and shape discrimination, the given number of detectors can be placed in specific azimuth angles around the 5°–10° scattering angle, such as 90°, 180°, and 270°.

Figure 5 shows the integrated scattering intensity versus the AF plots for the aerosol types described in

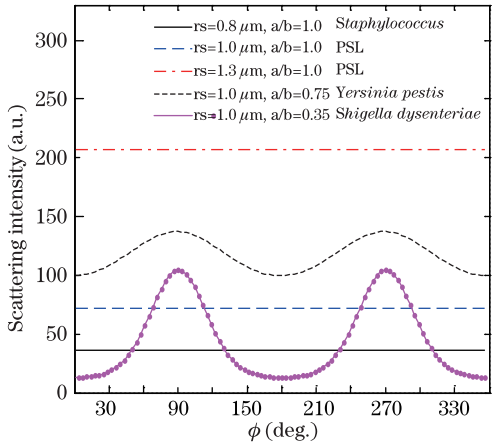

Fig. 4. Integrated scattering intensity within 5°–10° θ versus ϕ plots for aerosols of *Staphylococcus, Yersinia pestis, Shigella dysenteriae*, and PSL particles.

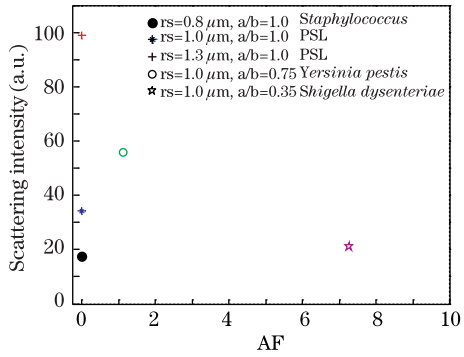

Fig. 5. Scattering intensity versus AF within 5°–10° θ plots at 0.589 μm wavelength for aerosols of S*taphylococcus, Yersinia pestis, Shigella dysenteriae*, and PSL particles.

Fig. 4. The results confirm that the scattering intensity is comparatively larger for larger equivalent size particles, making the distinction between particles with different sizes by scattering intensity alone feasible. For spherical particles, the 1.3-μm PSL shows a substantially larger value than the 1-μm PSL and 0.8-μm *Staphylococcus*. However, the scattering intensity of *Shigella dysenteriae* is lower than that of the *Yersinia pestis* particle due to the high non-sphericity of the former even if they have identical equivalent size.

As expected, AF values at a given scattering angle of perfectly spherical particles is zero. Moreover, the AF values are bigger than 0 and increase evidently as the non-sphericity increases for the *Yersinia pestis* and *Shigella dysenteriae* particles of lower aspect ratio. The PSL particles are clearly distinguishable from the non-spherical *Yersinia pestis* and *Shigella dysenteriae* particles, which exhibit AF values of ∼1.1 and ∼7.3, respectively. The oblate and prolate spheroids can produce the same AF values. Thus, to date, this method only pertains to the case where the general shape of the particles is known. Furthermore, in order to fully assess the degree of particle discrimination, it is essential to resort to extensive trials covering a wide variety of biological and nonbiological materials.

In conclusion, particle sizes and shapes can be discriminated through the analysis of the scattered light intensity distributions. The integrated scattering intensity in the 5°–10° scattering angle is proportional to the particle size, while the AF value is used to distinguish particles with different shapes. The combination of particle size and shape characterization from spatial scattering analysis offers a powerful method of classifying bioaerosol particles. The results can be used to aid in the designing of instruments that facilitate real-time bioaerosol particle detection.

This work was supported by the Important National Science and Technology Specific Projects of China (No. 2008ZX10401) and the Shanghai Municipal Natural Science Foundation (No. 11ZR1441700).

References

1. M. J. Shelton, S. P. Evans, P. D. Smith, I. A. Simpson, P. H. Kaye, and J. M. Clark, Proc. SPIE **5617,** 284 (2004).
2. A. Manninen, M. Putkiranta, A. Rostedt, J. Saarela, T. Laurila, M. Marjamäki, J. Keskinen, and R. Hernberg,

Appl. Opt. **47,** 110 (2008).
3. Y.-L. Pan, J. Hartings, R. G. Pinnick, S. C. Hill, J. Halverson, and R. K. Chang, Aerosol. Sci. Technol. **37,** 627 (2003).
4. P. H. Kaye, J. E. Barton, E. Hirst, and J. M. Clark, Appl. Opt. **39,** 3738 (2000).
5. P. P. Hairston, J. Ho, and F. R. Quant, J. Aerosol. Sci. **28,** 471 (1997).
6. C. Liang, H. Huang, and B. Ren, Acta Opt. Sin. (in Chinese) **25,** 1260 (2005).
7. E. Hirst and P. H. Kaye, J. Geophys. Res. **101,** 19231 (1996).
8. E. Hirst, P. H. Kaye, V. Foot, J. M. Clark, and P. B. Withers, Proc. SPIE **5617,** 416 (2004).
9. M. I. Mishchenko, J. W. Hovenier, and L. D. Travis, *Light Scattering by Nonspherical Particles: Theory, Measurements, and Applications* (Academic Press, San Diego, 2000).
10. M. I. Mishchenko, N. T. Zakharova, G. Videen, N. G. Khlebtsov, and T. Wriedt, J. Quant. Spectrosc. Radiat. Transfer **111,** 650 (2010).
11. M. G. Giacomelli, K. J. Chalut, J. H. Ostrander, and A. Wax, Opt. Lett. **33,** 2452 (2008).
12. M. A. Velazco-Roa, E. Dzhongova, and S. N. Thennadil, Appl. Opt. **47,** 6183 (2008).
13. A. M. K. Nilsson, P. Alsholm, A. Karlsson, and S. Andersson-Engels, Appl. Opt. **37,** 2735 (1998).
14. C. Lei, H. Liu, and H. Zhang, Acta Opt. Sin (in Chinese) **30,** 876 (2010).
15. P. H. Kaye, Meas. Sci. Technol. **9,** 141 (1998).
16. T. H. Jeys, W. D. Herzog, J. D. Hybl, R. N. Czerwinski, and A. Sanchez, Lincoln Lab. J. **17,** 29 (2007).
17. P. Foladori, A. Quaranta, and G. Ziglio, Water Res. **42,** 3757 (2008).
18. P. Latimer, A. Brunsting, B. E. Pyle, and C. Moore, Appl. Opt. **17,** 3152 (1978).
19. R. Xu, *Particle Characterization: Light Scattering Methods* (Kluwer Academic Publishers, Dordrecht, 2002).
20. P. Kaye, E. Hirst, and Z. Wang-Thomas, Appl. Opt. **36,** 6149 (1997).
21. H. Barthel, B. Sachweh, and F. Ebert, Meas. Sci. Technol. **9,** 210 (1998).
22. A. Borovoi, E. Naats, U. Oppel, and L. Grishin, Appl. Opt. **39,** 1989 (2000).
23. M. Giacomelli, Y. Zhu, J. Lee, and A. Wax, Opt. Express **18,** 14616 (2010).
24. B. A. Sachweh, W. D. Dick, and P. H. McMurry, Aerosol Sci. Technol. **23,** 373 (1995).